Signatures of spin-preserving symmetries in two-dimensional hole gases

Tobias Dollinger, Michael Kammermeier, Andreas Scholz, Paul Wenk, John Schliemann, and Klaus Richter
Institut für Theoretische Physik, Universität Regensburg, D-93040 Regensburg, Germany

R. Winkler
Department of Physics, Northern Illinois University, DeKalb, Illinois 60115, USA

(Received 29 April 2013; revised manuscript received 26 August 2014; published 15 September 2014)

We investigate ramifications of the persistent spin helix symmetry in two-dimensional hole gases in the conductance of disordered mesoscopic systems. To this end we extend previous models by going beyond the axial approximation for III-V semiconductors. For heavy-hole subbands we identify an exact spin-preserving symmetry analogous to the electronic case by analyzing the crossover from weak antilocalization to weak localization and spin transmission as a function of extrinsic spin-orbit interaction strength.

DOI: 10.1103/PhysRevB.90.115306 PACS number(s): 71.70.Ej, 72.25.Dc, 73.63.Hs

I. INTRODUCTION

Control over spin relaxation is essential to the operational capabilities of spin-based semiconductor devices [1,2]. A major advance in this respect has been the identification of an SU(2) symmetry that confines spin evolution to a characteristic topology and allows realizations of "persistent spin helix" (PSH) excitations which are robust against spin relaxation [2,3]. The latter could be identified by means of optical experiments [4,5] in two-dimensional electronic systems with linear-in-momentum Bychkov-Rashba [6] and Dresselhaus [7] type spin-orbit interaction (SOI) (here depending on the parameters α and β, respectively) of equal magnitude. As had already been suggested in Refs. [8,9], this symmetry at $\alpha = \pm\beta$ also becomes manifest in the weak localization (WL) feature in magnetoconductance traces of disordered materials with finite SOI, as opposed to weak antilocalization (WAL) mediated by spin relaxation [10]. Recent experiments confirmed theoretical predictions that the WL signature persists for n-doped systems even in the presence of non-negligible intrinsic SOI that scales with the cubic power of the wave number k [11–13]. The question naturally arises whether spin relaxation is also suppressed in p-doped semiconductors. Therefore, in the present work we investigate the generalization of the PSH symmetry arguments in the context of structurally confined heavy-hole (HH) states in III-V semiconductors forming a two-dimensional hole gas (2DHG). In these materials the spin is subject to strong SOI which typically enhance spin relaxation. This feature is mainly attributed to the carrier density dependence of the spin splitting, that has been investigated analytically by means of diagrammatic perturbation theory within the spherical approximation for one or more subbands [14]. Other works consider weak (anti-)localization in hole gases based on a semianalytical [15] as well as a semiclassical and numerical [16] treatment of 4×4 Luttinger-Kohn models [17].

II. TWO-DIMENSIONAL HOLE GAS MODEL

Here we focus on strong confinement described by an effective 2×2 model of the HH ground state. Our treatment is not restricted to the spherical or axial approximations, which significantly widens the range of observable phenomena compared to prior models. The low dimensionality allows for the identification of relevant symmetries that are used to deduce optimum parameter regimes for controlling spin relaxation. The structure of our model is given by the Hamiltonian

$$\mathrm{H} = \mathrm{H}_{\mathrm{kin}}\sigma_0 + \boldsymbol{\Omega}_{\mathrm{2DHG}} \cdot \boldsymbol{\sigma}, \tag{1}$$

where $\mathrm{H}_{\mathrm{kin}}$ denotes the kinetic energy, in which, to first approximation, the explicit dependence on the Luttinger parameters γ_i enters in the effective mass, $m_{\mathrm{eff}} \approx m_0/(\gamma_1 + \gamma_2)$, where m_0 is the mass of the free electron and we have assumed a 2D system on a (001) surface [18]. Here σ_0 is the identity matrix, $\boldsymbol{\sigma}$ the vector of Pauli matrices, and $\boldsymbol{\Omega}_{\mathrm{2DHG}}$ the effective spin-orbit field coupling to the spin. All boldface symbols used in the present text denote 2D vectors with only xy components. In contrast to the corresponding expression for electrons, $\boldsymbol{\Omega}_{\mathrm{2DEG}}$, where k-linear terms are dominant [9], to leading order $\boldsymbol{\Omega}_{\mathrm{2DHG}}$ is characterized by a cubic momentum dependence. This is in agreement with existing 2DHG models and results from coupling of the HH to the light hole (LH) subbands [19–21]. The result (1) is obtained via a perturbation expansion of the standard Luttinger-Kohn Hamiltonian [17] in the basis given by the subband edge states [18]. Our model applies to typical zinc-blende structure materials, as can be inferred from their material properties and calculated band structures given, e.g., in Ref. [18]. In Eq. (1), the 2×2 Hamiltonian H represents the subspace spanned by the HH states of spin angular momenta $\pm(3/2)\hbar$. The corresponding hole spin-orbit field is given by

$$\begin{aligned}\boldsymbol{\Omega}_{\mathrm{2DHG}} = \beta_{\mathrm{HH}}\boldsymbol{k} + \lambda_{\mathrm{D}}\big\{ &- \bar{\gamma}\boldsymbol{k}^2\boldsymbol{k} + \delta\big[k_x^3\hat{\boldsymbol{x}} + k_y^3\hat{\boldsymbol{y}} \\ &- 3k_xk_y(k_y\hat{\boldsymbol{x}} + k_x\hat{\boldsymbol{y}})\big]\big\} + \lambda_{\mathrm{R}}\big\{\delta\boldsymbol{k}^2(k_y\hat{\boldsymbol{x}} + k_x\hat{\boldsymbol{y}}) \\ &+ \bar{\gamma}\big[- k_y^3\hat{\boldsymbol{x}} - k_x^3\hat{\boldsymbol{y}} + 3k_xk_y\boldsymbol{k}\big]\big\},\end{aligned} \tag{2}$$

with the intrinsic Dresselhaus parameters

$$\beta_{\mathrm{HH}} = -\frac{\sqrt{3}C_k}{2}, \tag{3}$$

$$\lambda_{\mathrm{D}} = \frac{\sqrt{3}\hbar^2}{2m_0\Delta_{\mathrm{HL}}}\big[C_k + \sqrt{3}\widetilde{b_{41}^{8v8v}}\,\langle k_z^2\rangle\big], \tag{4}$$

the structural, electrical field $\langle E_z \rangle$ dependent Bychkov-Rashba parameter,

$$\lambda_R = \frac{3\hbar^2}{2m_0\Delta_{HL}}\langle E_z \rangle \widetilde{r_{41}^{8v8v}}, \tag{5}$$

and the Luttinger parameters $\bar{\gamma} = (\gamma_3 + \gamma_2)/2$ and $\delta = (\gamma_3 - \gamma_2)/2$ as in Ref. [22]. Here C_k is a material constant while $\widetilde{r_{41}^{8v8v}}$ and $\widetilde{b_{41}^{8v8v}}$ are parameters which depend on both material properties and geometry. In the bulk case the latter two parameters coincide with r_{41}^{8v8v} and b_{41}^{8v8v}, respectively, consistent with Ref. [18]. In the presence of a confinement, these parameters are modified. Since the value b_{41}^{8v8v} is mainly defined by the valence band (Γ_{8v}) and conduction band (Γ_{6c}) gap E_0, this type of Dresselhaus contribution is hardly affected by the subband quantization. Thus we assume $b_{41}^{8v8v} \approx \widetilde{b_{41}^{8v8v}}$. This does not hold for the dominant contribution by Rashba SOI, because the origin of the SOI, which is connected with the coefficient $\widetilde{r_{41}^{8v8v}}$, changes: in the presence of the confinement, the contribution due to Rashba SOI in the effective HH system is dominated by the subband splitting between HH and LH. This dominant contribution is proportional to the term which is denoted here by $\widetilde{r_{41}^{8v8v}}$. The contribution described by r_{41}^{8v8v}, though, is induced by the coupling between valence and conduction bands: it represents a higher order correction and will not be considered in the following [23]. Previous models [20,21,24] focus on the axially symmetric situation, $\delta = 0$. The above expression represents a generalization of these models, allowing for the description of a broader range of materials and considering anisotropies that are important, for instance, in the plasmon spectra of HH systems [25]. Vertical confinement is modeled by a potential well with perpendicular wave number $\langle k_z^2 \rangle$ that displays a splitting $\Delta_{HL} = 2\gamma_2\hbar^2\langle k_z^2 \rangle/m_0$ between HH and LH bands. For further analysis, the terms proportional to the small parameter C_k are neglected in Eqs. (3) and (4), since for realistic materials and large wave vectors (densities), the physics is dominated by the terms proportional to $b_{41}^{8v8v}\langle k_z^2 \rangle$, as shown in Table 6.3 in Ref. [18]. Furthermore, the linear Dresselhaus term (3) effectively rescales the axially symmetric part of the cubic Dresselhaus contribution. Equation (2) results from sequential perturbation expansions up to third order in k and to first order with respect to the inverse splitting ${\Delta_{HL}}^{-1}$ and to E_z imposed on the crystal. The identification of enhanced spin relaxation times in this work is closely connected with broken axial symmetry, since here a conserved quantity related to the spin degree of freedom can only be constructed in the presence of terms with both two- and threefold rotational symmetry in the extrinsic and the intrinsic SOI. Our findings suggest that obtaining an exact PSH symmetry is limited by the parameters of realistic systems, since it requires that $\gamma_3 = 0$. Although an approximate symmetry in the leading-order Fourier components of Ω_{2DHG} causes a weakly perturbed crossover from WAL to WL, similar to electronic systems with cubic intrinsic SOI [11], reaching exact spin preservation associated with $\gamma_3 = 0$ is not realistic. This is due to the relation of the Kohn-Luttinger parameters described in Ref. [26], which causes γ_2 to vanish in the given case. This however violates the perturbation expansion, in which the small parameter scales as γ_2^{-1}. The influence of strain on our above discussed model has been discussed in Ref. [27], in which the persistent spin evolution requires the condition $\gamma_2 = -\gamma_3$. This criterion is not realizable for the above mentioned reasons. In the present discussion we will also focus on the realization of long-lived, but not fully preserved spin states in effective heavy-hole models, for a suitable choice of the ratio γ_2/γ_3. In contrast, for $\eta = -1$ and $\gamma_3 = 0$, as investigated in Fig. 2, the fully symmetric situation is obtained, corresponding to principally infinite spin lifetimes.

III. CHARGE TRANSPORT ANALYSIS

A. Persistent spin helix conditions

The effect of the spin symmetry on the magnetoconductance $G(B)$ can be analyzed by formulating the transmission in the Landauer-Büttiker framework [28,29],

$$\frac{h}{e^2}G = \left(\sum_{n,m;\sigma=\sigma'} + \sum_{n,m;\sigma\neq\sigma'} \right) |t_{n\sigma,m\sigma'}|^2 =: T_D + T_{OD}, \tag{6}$$

according to the spin quantum numbers σ,σ' in terms of diagonal spin-preserving channels T_D and spin off-diagonal contribution T_{OD}. Here, $\sigma,\sigma' = \pm 1$ refer to an arbitrary basis defined in the ballistic leads of a two-terminal device representing our numerical model, while n,m are integers that define the transverse channel of the in- and outgoing states due to a hard-wall confinement defining the edges of the leads. The lead wave functions $|\phi_{n,\sigma}\rangle$ and $|\phi_{m,\sigma'}\rangle$ enter into the Fisher-Lee relation for the amplitudes

$$t_{n\sigma,m\sigma'} \propto \int_{\partial \text{ leads}} d^2r \langle \phi_{n,\sigma}|y_1\rangle\langle y_1|G_R|y_2\rangle\langle y_2|\phi_{m,\sigma'}\rangle, \tag{7}$$

where the integration is taken over the lead cross sections [30]. $G_R = (E_F - H + 0_+)^{-1}$ is the Green's function of the scattering region at fixed Fermi energy E_F. Knap *et al.* [9] found in n-type systems particular relations between extrinsic and intrinsic SOI magnitude, for which the Cooperon becomes separable and a WL signal rather than WAL is observed. In terms of the structure provided by Eq. (6), T_{OD} vanishes in this case and correspondingly spin scattering is absent even in transport in disordered systems. This is equivalent to the observation that the system displays an exact, disorder independent symmetry [2,3], which allows for a decomposition within the corresponding constant eigenbasis $\{|\chi_\sigma\rangle\}$ into $\mathbf{\Omega}\cdot\boldsymbol{\sigma} = \sum_{\sigma=\pm1} E_\sigma(\mathbf{\Omega})|\chi_\sigma\rangle\langle\chi_\sigma|$. Hence, when taking the spin trace in Eq. (6) in the basis $\{|\chi_\sigma\rangle = (1,\sigma\ \exp[\pm i\pi/4])^\dagger\}$, corresponding to the existence of the conserved quantity $\Sigma_\pm = \sigma_x \pm \sigma_y$ or, equivalently, fixed in-plane spin orientation along $\varphi = \pm\pi/4$, one finds that

$$T_{OD} \propto \sum_{\sigma\neq\sigma'} |\langle\chi_\sigma|\chi_{\sigma'}\rangle|^2 = \sum_{\sigma\neq\sigma'} \delta_{\sigma,\sigma'} \tag{8}$$

is suppressed and T_D decomposes into two independent channels which trivially display WL [9]. In the hole model (2) we find the analog to the electronic PSH symmetry if the system parameters fulfill $\eta = \pm 1$ and $\bar{\gamma} = -\delta$, i.e., $\gamma_3 = 0$, where we define the parameter $\eta \equiv \lambda_R/\lambda_D$. In these two cases the direction of $\mathbf{\Omega}_{2DHG}$ is fixed independently of the

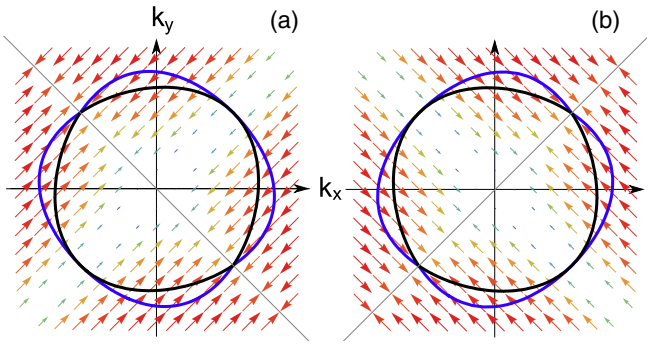

FIG. 1. (Color online) Fermi surface for the different spin directions obtained from Eq. (1) (black and blue (gray) contours) and the corresponding direction of the effective spin-orbit field, $\mathbf{\Omega}_{\mathrm{2DHG}}$, illustrated by arrows. The SOI parameters establish a persistent spin helix for holes with uniaxial spin orientation corresponding to $\eta \equiv \lambda_{\mathrm{R}}/\lambda_{\mathrm{D}} = +1$ (a) and $\eta = -1$ (b). In both cases the Luttinger parameters are $\bar{\gamma} = -\delta$, i.e., $\gamma_3 = 0$.

momentum, more precisely by

$$\mathbf{\Omega}_{\mathrm{2DHG}} \propto \left[-\boldsymbol{k}^2(k_x \pm k_y) \pm 3k_x k_y(k_x \pm k_y) - k_x^3 \mp k_y^3\right](\hat{\boldsymbol{x}} \pm \hat{\boldsymbol{y}}). \quad (9)$$

We illustrate these cases in Fig. 1, where the effective spin-orbit field $\mathbf{\Omega}_{\mathrm{2DHG}}$ is oriented along a fixed direction for both spin split subbands. The structure of Eq. (2) implies an additional symmetry for $\bar{\gamma} = \delta$, which is however outside the range of validity, since it corresponds to $\gamma_2 = 0$ and thereby a breakdown of perturbation theory. Although the given parameters can be engineered in realistic material systems, as indicated by Table C.9 in Ref. [18], it is not possible to influence the effective values of γ_3, without simultaneously changing γ_2 or the effective values of the Rashba and Dresselhaus coefficients [26].

B. Numerical setup

To investigate the previously described properties we simulate transport in disordered hole systems connected to two terminals, represented by ballistic semi-infinite leads without SOI. The latter is switched on and off adiabatically over one-fifth of the total length of a rectangular scattering region to which the leads are connected. We use an average over an Anderson-like uniformly distributed random-box potential V_{dis} to simulate disorder. The perpendicular magnetic field is included by means of Peierls' substitution. The Hamiltonian is then discretized on a tight-binding grid in position space and the transmission amplitudes are obtained by an optimized recursive Green's function algorithm [31]. Since we are interested in modeling bulk transport, we implemented periodic boundary conditions in the transverse direction to minimize effects from the boundaries.

C. PSH signatures in the magnetoconductance

The symmetry condition becomes apparent in the magnetoconductance of disordered 2DHG systems, as illustrated in Fig. 2. Here we show results of the numerically calculated disorder averaged transmission, Eq. (6), for finite cubic

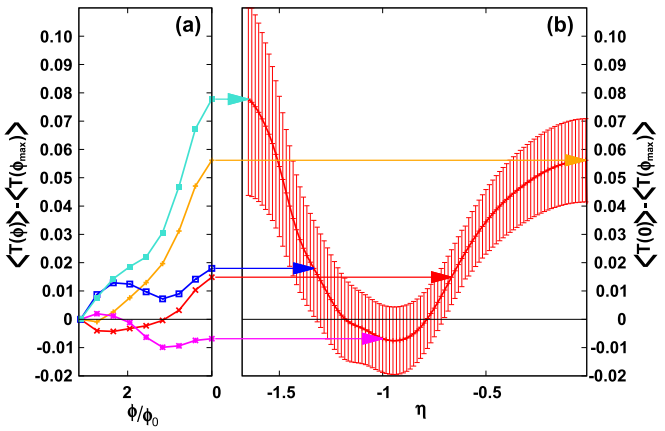

FIG. 2. (Color online) Signatures of spin-preserving symmetries in weak localization of a two-dimensional hole gas. (a) Disorder-averaged magnetoconductance correction $\langle T(\phi)\rangle - \langle T(\phi_{\max})\rangle$ as a function of flux ϕ (in units of $\phi_0 = h/e$; $\phi_{\max}/\phi_0 = 3.1$) for spin-orbit coupling ratios $\eta \equiv \lambda_{\mathrm{R}}/\lambda_{\mathrm{D}} = -1.65, -0.017, -1.33, -0.67, -1$ (from top to bottom). (b) Conductance correction $\langle T(0)\rangle - \langle T(\phi_{\max})\rangle$ as a function of η. Negative magnetoconductance reflects suppression of spin relaxation close to $\eta = -1$. System parameters: disorder average over 1000 impurity configurations for a scattering region of aspect ratio (length L to width W) 200:80 unit cells with periodic boundary conditions in transverse direction. Quantum transmission computed for $k_{\mathrm{F}}W/\pi = 13$ hole states per spin supported in the leads, elastic mean free path $l = 0.04W$, $\gamma_3 = 0$, and fixed Dresselhaus spin precession length $k_{\mathrm{D}}W \approx 1$, defined below Eq. (18).

intrinsic SOI λ_{D} as a function of the extrinsic SOI λ_{R}. For demonstrative purposes, we set $\gamma_3 = 0$. Representative examples of the conductance correction traces are shown in Fig. 2(a), which display typical WAL and WL line shapes as a function of magnetic flux ϕ from a homogeneous magnetic field perpendicular to the 2DHG plane. Considering the dependence on η, we find pronounced signatures of WAL if η is far from -1. When η approaches -1, a crossover from WAL to WL occurs as indicated by a maximum negative conductance correction, in agreement with the symmetry argument. In Fig. 2(b) our results are summarized in terms of the conductance at maximum magnetic flux $\langle T(\phi_{\max})\rangle$ subtracted from the correction at zero flux $\langle T(0)\rangle$ plotted as a function of η, where we chose $\phi_{\max} = 3.1\phi_0$. The results show that the parameter regime where a PSH type symmetry occurs is characterized by a negative conductance correction, i.e., by a WL signature.

D. Diagrammatic approach

1. Cooperon of the effective 2DHG

Our analysis above is confirmed within a diagrammatic perturbative treatment by exact diagonalization of the Cooperon $\hat{C}(\mathbf{Q})$ in the framework of the effective model (1). For this purpose, the scheme presented in Refs. [32,33] for electrons is generalized to holes. The diagrammatic approach is justified since we assume the system to be in the diffusive regime fulfilling the Ioffe-Regel criterion, $E_{\mathrm{F}}\tau/\hbar \gg 1$, with elastic scattering time τ and Fermi energy E_{F}. Here the scattering is modeled by standard "white-noise" disorder $V(\mathbf{x})$

which vanishes on average, $\langle V(\mathbf{x})\rangle = 0$, and is uncorrelated, $\langle V(\mathbf{x})V(\mathbf{x}')\rangle = \delta(\mathbf{x}-\mathbf{x}')/(2\pi\nu\tau/\hbar)$, where ν is the density of states per spin channel. Unfortunately, a general analytical study of the Cooperon of the confined 2DHG including both the SOI due to BIA and SIA is spoiled by the fact that this operator, which is necessary to describe the conductivity correction due to interference between a $J = 3/2$ hole and its time-reversed counterpart, requires 16 dimensions. However, since we mapped the 4×4 Luttinger Hamiltonian onto an effective one considering only the spin $\pm 3/2$ subspace, the Cooperon of this effective model is equivalent to the Cooperon of s-band conduction electrons presented in Refs. [32,33], except for the absolute value of the spin and the terms appearing due to SOI. The total Cooperon momentum $\mathbf{Q}$ is the sum of the momenta of the retarded and advanced propagators of holes, $\mathbf{Q} = \boldsymbol{k} + \boldsymbol{k}'$. Their spins $(3/2)\hbar\boldsymbol{\sigma}$ and $(3/2)\hbar\boldsymbol{\sigma}'$ sum up to $\mathbf{S} = (3/2)\hbar(\boldsymbol{\sigma}+\boldsymbol{\sigma}')$. We get to second order in $[\hbar\mathbf{Q} + (2/3)m_{\mathrm{eff}}\hat{a}\mathbf{S}]$ and after an angular average $\langle\cdots\rangle_\varphi$ over the Fermi surface

$$\hat{C}(\mathbf{Q}) = \frac{\hbar}{D_h\left(\hbar\mathbf{Q} + \frac{2}{3}m_{\mathrm{eff}}\langle\hat{a}\rangle_\varphi\cdot\mathbf{S}\right)^2 + H_\gamma}, \tag{10}$$

where $D_h = \tau v_{\mathrm{F}}^2/2$ is the diffusion constant. The matrix $\hat{a}$ in the effective vector potential term is defined by the relation $\boldsymbol{\sigma}\cdot\boldsymbol{\Omega}_{\mathrm{2DHG}} = \boldsymbol{k}\cdot(\hat{a}\cdot\boldsymbol{\sigma})$. With $\langle\hat{a}\rangle_\varphi \equiv \hat{\alpha}$ we find

$$\hat{\alpha} = \frac{m_{\mathrm{eff}}}{2\hbar^4}E_{\mathrm{F}}\begin{pmatrix}\lambda_{\mathrm{D}}(3+c_{\mathrm{D}}) & \lambda_{\mathrm{R}}(3+c_{\mathrm{R}})\\ \lambda_{\mathrm{R}}(3+c_{\mathrm{R}}) & \lambda_{\mathrm{D}}(3+c_{\mathrm{D}})\end{pmatrix}, \tag{11}$$

with $E_{\mathrm{F}} = m_{\mathrm{eff}}v_F^2/2$ the Fermi energy, $c_{\mathrm{D}} = 2\gamma_3/\gamma_2 - 1$, and $c_{\mathrm{R}} + c_{\mathrm{D}} = -2$. The term

$$H_\gamma = \frac{1}{9}\frac{D_h m_{\mathrm{eff}}^4 E_{\mathrm{F}}^2}{\hbar^8}\left[\left(\lambda_{\mathrm{D}}^2(c_{\mathrm{D}}-1)^2 + \lambda_{\mathrm{R}}^2(c_{\mathrm{R}}-1)^2\right)\times\left(S_x^2+S_y^2\right) + 2(c_{\mathrm{D}}-1)(c_{\mathrm{R}}-1)\lambda_{\mathrm{R}}\lambda_{\mathrm{D}}\{S_x,S_y\}\right] \tag{12}$$

is $\mathbf{Q}$ independent and resembles the corresponding expression for the 2DEG in Ref. [32] which appears due the existence of cubic Dresselhaus SOI. We simplify the calculation by assuming $\beta/\lambda_{\mathrm{D}}$ to be negligibly small and by rescaling the Cooperon Hamiltonian $H_{\mathrm{C}} \equiv \hat{C}^{-1}$ for nonzero intrinsic Dresselhaus λ_{D}:

$$\tilde{H}_{\mathrm{C}} \equiv \frac{H_{\mathrm{C}}}{D_h\left(\lambda_{\mathrm{D}}\frac{m_{\mathrm{eff}}^2}{3\hbar^3}E_{\mathrm{F}}\right)^2} \tag{13}$$

$$= \begin{pmatrix}\hbar\tilde{Q}_x + \hbar^{-1}[(3+c_{\mathrm{D}})S_x + \eta(1-c_{\mathrm{D}})S_y]\\ \hbar\tilde{Q}_y + \hbar^{-1}[(3+c_{\mathrm{D}})S_y + \eta(1-c_{\mathrm{D}})S_x]\end{pmatrix}^2 + \hbar^{-2}[(1-c_{\mathrm{D}})^2 + \eta^2(3+c_{\mathrm{D}})^2]\left(S_x^2+S_y^2\right) + 2\hbar^{-2}(1-c_{\mathrm{D}})(3+c_{\mathrm{D}})\eta\{S_x,S_y\}, \tag{14}$$

with $\tilde{Q}_i = Q_i/\lambda_{\mathrm{D}}\frac{m_{\mathrm{eff}}^2}{3\hbar^3}E_{\mathrm{F}}$. Since the spectra of the Cooperon and Diffuson are equal as long as time reversal symmetry is not broken, the term H_γ, which cannot be rewritten as a vector potential, causes in general gaps in the triplet sector of the spectrum which correspond to finite spin relaxations [33]. As in the case of 2DEG, only the triplet sector is affected by SOI [here, due to the effective HH model, we have $S = (3/2+3/2)\hbar$ but one can use $\{|S=0,m=0\rangle, |S=1,m=1\rangle, |S=1,m=0\rangle, |S=1,m=-1\rangle\}$ as a basis since $\mathbf{S}\sim(\boldsymbol{\sigma}+\boldsymbol{\sigma}')$]. The appearance of gapless modes besides the singlet mode, i.e., the existence of persistent spin states as found by using the Landauer-Büttiker framework, will be discussed in the following.

2. *Persistent and long-lived spin states*

We focus on two interesting parameter regimes: Luttinger parameters which describe systems close to axial symmetry where we have $c_{\mathrm{D}} \approx 1$ and the extreme case $c_{\mathrm{D}} = -1$ for which the SO field $\Omega_{\mathrm{2DHG}}(\mathbf{k})$ is aligned in one direction if $|\eta| = 1$ as presented in Fig. 2.

An analysis of the Cooperon triplet spectrum for values $c_{\mathrm{D}} \approx 1$ and moderate strength of Rashba SOI, i.e., $-\sqrt{3} \leqslant \eta \leqslant \sqrt{3}$, reveals that the absolute minimum expressed in polar coordinates as $\tilde{\mathbf{Q}} = (\tilde{Q},\varphi)$ can be found at finite $\tilde{Q}_{\mathrm{min}} = \sqrt{3(3-\eta^2)(5+\eta^2)}$ with an energy of

$$\tilde{E}_{\mathrm{min},1}(\tilde{Q}_{\mathrm{min}}) = 21 + 66\eta^2 - 3\eta^4 + \tfrac{3}{2}\lambda[\eta(5+6\eta^2+\eta^4)\times\sin(2\varphi) - 7 - 22\eta^2 + \eta^4] + O(\lambda^2), \tag{15}$$

with $\lambda = 1 - c_{\mathrm{D}}$ and $|\lambda| \ll 1$. Thus the spectrum will always be gapped with a minimal gap for $\eta = 0$. The spin states to which the minima correspond are long-lived (finite spin relaxation) modes which describe a spin helix due to $\tilde{Q}_{\mathrm{min}} > 0$ [33]. The situation differs completely for the case where the Luttinger parameter γ_3 vanishes, i.e., $c_{\mathrm{D}} = -1$. We find an absolute minimum of the Cooperon triplet spectrum at $\tilde{Q} = 0$ with

$$\tilde{E}_{\mathrm{min},-1}(\tilde{Q}) = 24(1-|\eta|)^2 + \tfrac{1}{4}\tilde{Q}^2[(3-|\eta|)(1+|\eta|) + (1-|\eta|)^2\sin(2\varphi)] + O(\tilde{Q}^3), \tag{16}$$

for $|\eta| \approx 1$. As a consequence, we obtain a gapless mode for $|\eta| = 1$. This supports the numerical findings of persistent spin states if the aforementioned symmetries are present: changing η from $\eta = 0$ to $\eta = -1$ as done in Fig. 2, we see that the energetically lowest mode, Eq. (16), is gapped at $\eta = 0$. Thus the negative contribution of the triplet modes to the conductivity correction $\Delta\sigma = (W/L)(e^2/h)\langle T(0)\rangle - \langle T(\phi_{\mathrm{max}})\rangle$ is suppressed and we end up with an enhancement of conductivity (WAL) stemming from the positive gapless singlet channel. Enhancing $|\eta|$ does not change the singlet-mode contribution to $\Delta\sigma$. However, the suppression of triplet contribution is reduced: we see a reduction of conductivity leading to WL in the case where in addition to the gapless singlet mode a gapless triplet mode appears.

IV. SPIN TRANSPORT ANALYSIS

Apart from considering the indirect influence of the PSH symmetry on the WL-WAL transition, it seems natural to search for a manifestation of a symmetry in T_{D}, Eq. (6), since its effects could be determined by magnetic polarization of the leads, allowing for spin transistor operation even in the presence of disorder [2]. Numerically we can confirm the validity of the latter approach by calculating the normalized quantity $T_{\mathrm{D}}/(T_{\mathrm{D}}+T_{\mathrm{OD}})$ as a function of $\eta = \lambda_{\mathrm{R}}/\lambda_{\mathrm{D}}$, as shown in Fig. 3.

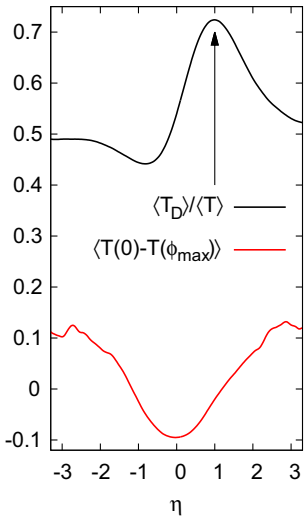

FIG. 3. (Color online) Top: ratio of disorder averaged diagonal transmission over total transmission $\langle T_{\rm D}\rangle/\langle T\rangle = \langle T_{\rm D}\rangle/\langle T_{\rm D} + T_{\rm OD}\rangle$ as a function of η for a scattering region with 150:80 aspect ratio for fixed Dresselhaus spin precession length $k_{\rm D}^{-1} \approx (k_F^2\lambda_D)^{-1} = 1.3W$ and Luttinger parameters $\gamma_2 = 1$ and $\gamma_3 = 0.25$ for which no exact spin-preserving symmetry can be established. The peak of $\langle T_{\rm D}\rangle/\langle T\rangle$ at $\eta = 1$ (indicated by the arrow), coincides with the maximum of the diabatic transition probability of Eq. (18). Average transmission shown includes 1000 disorder configurations. With respect to the eigenbasis of $\eta = -1$, we obtain a curve that coincides with the mirror image of the shown plot, displaying a maximum at $\eta = -1$. Bottom: amplitude of the magnetoconductance correction in which no WAL-WL-WAL transition is observable in the vicinity of the symmetry point of $|\eta| = 1$ due to insufficient spin randomization in the regime $|\eta| < 1.19$. This example indicates that in a sweep of the Rashba SOI, the point where Rashba and Dresselhaus SOI are balanced displays a clear signal in the diagonal transmission, while it may not be detectable in the form of a WAL-WL-WAL transition.

We identify a pronounced transmission maximum at $\eta = 1$ in the basis corresponding to the $+\pi/4$ spin orientation even in situations where the exact PSH-type symmetry is not realized. In the given example we chose the Luttinger parameters $\gamma_2 = 1$ and $\gamma_3 = 0.25$ which correspond to arbitrarily chosen parameters, that serve as a proof of concept of measurements in a setup, where a WAL-WL-WAL transition upon variation of the Rashba SOI is not experimentally observable. For values of $|\eta| < 1.19$, the conductance correction corresponding to Fig. 3 is still dominated by WL, corresponding to insufficient spin randomization. For $|\eta| > 1.19$ we observe WAL, consistent with the increased magnitude of the SOI. Therefore, the experimental determination of the relative magnitude of Rashba and Dresselhaus SOI from the WAL-WL-WAL transition is not feasible in this setup, because the point where both contributions are in balance, i.e., $|\eta| = 1$, lies within the regime of small spin randomization. In the spin-resolved transmission signal the symmetry point is however clearly visible, as demonstrated by the maximum in Fig. 3. For parameters far from $\eta = 1$ the spin transmission is equally distributed among the diagonal and off-diagonal channels. When $|\eta|$ approaches unity, $T_{\rm D}$ formally corresponds to the probability of diabatic Landau-Zener transitions between instantaneous eigenstates $|\pm\mathbf{\Omega}\rangle = (1, \pm\exp[-i\ \arctan(\Omega_y/\Omega_x)])^\dagger$ of the spin-orbit contribution (2). The momentum direction is changed by disorder scattering such that the spin evolution is subject to inhomogeneities of the effective spin-orbit field $\mathbf{\Omega}$. At the minima of the anisotropic spin splitting $2|E_\sigma(\mathbf{\Omega})|$, this induces transitions of the type $|\pm\mathbf{\Omega}\rangle \to |\mp\mathbf{\Omega}\rangle$ with Landau-Zener [34,35] transition probability

$$P_{\rm D} = \exp\left[-2\pi\epsilon_{12}^2/(\hbar|\partial_t(\epsilon_1(t) - \epsilon_2(t))|)\right]. \qquad (17)$$

The value of $P_{\rm D}$ is calculated from the minimal spin splitting, $2\epsilon_{12}$, in the corresponding directions $\varphi := \arctan(k_y/k_x)$ and the slope of the splitting, $\epsilon_1(t) - \epsilon_2(t)$, between the fully diabatically coupled basis states.

These transitions enhance the value of $T_{\rm D}$ while completely suppressing $T_{\rm OD}$ for $P_{\rm D} = 1$. The spinors $\{|\chi_\sigma\rangle\}$ underlying Eq. (6) coincide with the diabatic superposition of the states $|\pm\mathbf{\Omega}\rangle$. The latter can be checked by considering $\langle\chi_\sigma|\mathbf{\Omega}\cdot\boldsymbol{\sigma}|\chi_\sigma\rangle$. Within the HH model (2) the diabatic basis coincides with that of the PSH eigenstates $\{|\chi_\sigma\rangle\}$ of a 2DEG [2]. For p-type systems we find a probability of

$$\ln(P_{\rm D})_{\rm 2DHG} = -\zeta l|k_{\rm D}||\bar\gamma + \delta|(1 - |\eta|)^2, \qquad (18)$$

with the elastic mean free path l and a phenomenological factor ζ of order 1, related to the details of the scattering. These quantities enter together with the transport time τ into the rate of change in angle φ in the relation $\delta\varphi = \pi\delta t/(2\tau\zeta)$. The characteristic length scale of spin precession $k_{\rm D}^{-1}$ is approximated as $k_{\rm D} \approx k_{\rm F}^2\lambda_{\rm D}$. Equation (18) is derived under the assumption that $\bar\gamma \neq -\delta$. Although the expression (17) for the Landau-Zener transition probability predicts a clear maximum at $|\eta| = 1$, Eq. (18) does not cover the description of $T_{\rm D}$ for parameters where the PSH symmetry is established. It is nevertheless applicable to realistic material parameters if $\gamma_3 \neq 0$ and, consequently, $\bar\gamma \neq -\delta$, which is verified by a numerical transport analysis. The analysis of $T_{\rm D}$ can be applied to electronic systems as well, with an effective spin-orbit field,

$$\mathbf{\Omega}_{\rm 2DEG} = \alpha\boldsymbol{k}\times\hat{\boldsymbol{z}} + \beta(k_x\hat{\boldsymbol{x}} - k_y\hat{\boldsymbol{y}}) + \gamma\left(-k_xk_y^2\hat{\boldsymbol{x}} + k_yk_x^2\hat{\boldsymbol{y}}\right), \qquad (19)$$

for transport along the [100] direction in a 2DEG grown in [001] direction and with $\langle k_z^2\rangle\gamma = \beta$ [9]. In systems described by this model the corresponding Landau-Zener transition probability is given by

$$\ln(P_{\rm D})_{\rm 2DEG} = -\zeta l|k_\beta|(\Gamma_\beta/2 - 1 \pm \eta)^2, \qquad (20)$$

with the Dresselhaus spin precession length $k_\beta^{-1} = (m_{\rm eff}\beta/\hbar^2)^{-1}$, ratio of cubic and linear SOI $\Gamma_\beta = k_{\rm F}^2\gamma/\beta$, and the phenomenological factor ζ as it appears in Eq. (18). This model has been verified by numerical calculations which are beyond the scope of this work. In both p- and n-type systems, the signatures in $T_{\rm D}$ are robust against disorder.

Therefore, as an experimental approach to analyzing spin relaxation lengths in transport within HH systems, a detection of the PSH signature in the longitudinal conductance of a spin-polarized current is favorable. The mechanism responsible for the peaks in $T_{\rm D}$ is the momentum space analog to the effect of a spatially inhomogeneous helix-type Zeeman term on the spin conductance in dilute magnetic semiconductors [36]. An alternative measurement method for further investigation of

the HH PSH is represented by magneto-optical Kerr rotation techniques, which recently allowed one to map the spin topology in electronic systems [5].

ACKNOWLEDGMENTS

We acknowledge financial support by Deutsche Forschungsgemeinschaft (DFG) within the collaborative research center SFB 689 and by the Elitenetzwerk Bayern (T.D.). We thank J. Fischer and V. Krückl for helpful discussions, and M. Wimmer for providing the numerical algorithm used here.

APPENDIX: DIABATIC TRANSITIONS IN MOMENTUM SPACE

To obtain the leading-order contribution to the spin-diagonal transmission defined in Eqs. (18) and (20), we start from the diagonal approximation to the semiclassical transmission amplitudes [37],

$$T_{\sigma,\sigma} \sim \sum_{\gamma} |A_\gamma|^2 |\langle\sigma|\mathrm{D}_\gamma|\sigma\rangle|^2, \tag{A1}$$

with the stability amplitude $|A_\gamma|^2$ corresponding to classical paths γ that connect the incident lead with the outgoing lead for the respective channels. Summing the above expression with respect to the spin polarizations $\sigma = \pm 1$ yields the semiclassical leading-order contribution to T_D after performing a disorder average. Without the spin evolution kernel D, the Drude conductance can be estimated from Eq. (A1), since the summation over the amplitudes can be expressed in terms of classical transmission probabilities [38]. For small spin splitting compared to the kinetic energy, the trajectories γ are solely determined by classical properties of the system. They parametrize the spin dynamics via the equation for the spin evolution kernel along the path γ [37],

$$i\hbar\frac{\partial}{\partial t}\mathrm{D}_\gamma(t)|\sigma\rangle = \boldsymbol{\Omega}(\boldsymbol{k}(t))\cdot\boldsymbol{\sigma}\,\mathrm{D}_\gamma(t)|\sigma\rangle, \tag{A2}$$

for the effective spin-orbit field $\boldsymbol{\Omega}$ for electrons, Eq. (19), or holes, Eq. (2), respectively. To estimate for which values of the spin-orbit parameters the value of $T_{\sigma,\sigma}$ reaches a maximum, we calculate $|\langle\sigma|D_\gamma(t)|\sigma\rangle|^2$ from Eq. (A2) as the probability to remain in the instantaneous eigenstate matching the initial polarization at the lead-cavity interface via the Landau-Zener formula [34,35]. We specified the time-dependent problem (A2) after disorder average by a momentum $\boldsymbol{k}(t) \approx k(\cos\varphi(t)\hat{\boldsymbol{x}} + \sin\varphi(t)\hat{\boldsymbol{y}})$ that changes due to elastic small-angle scattering according to $\delta\varphi = \pi\delta t/(2\tau\zeta)$. Here we introduce the phenomenological parameter ζ by hand. $\zeta = 1$ corresponds to a momentum change due to isotropic scattering and τ is the elastic momentum relaxation time. Note that the disorder model on which the numerical results of Fig. 3 are based consists of Anderson-like impurity configurations with small correlation lengths. Although the semiclassical picture presented above is not applicable to this setup in a strict sense, it describes the observed behavior remarkably well.

[1] I. Žutić, J. Fabian, and S. Das Sarma, Rev. Mod. Phys. **76**, 323 (2004).
[2] J. Schliemann, J. C. Egues, and D. Loss, Phys. Rev. Lett. **90**, 146801 (2003).
[3] B. A. Bernevig, J. Orenstein, and S.-C. Zhang, Phys. Rev. Lett. **97**, 236601 (2006).
[4] J. D. Koralek, C. P. Weber, J. Orenstein, B. A. Bernevig, S.-C. Zhang, S. Mack, and D. D. Awschalom, Nature (London) **458**, 610 (2009).
[5] M. P. Walser, C. Reichl, W. Wegscheider, and G. Salis, Nat. Phys. **8**, 757 (2012).
[6] E. I. Rashba, Sov. Phys. Solid State **2**, 1109 (1960).
[7] G. Dresselhaus, Phys. Rev. **100**, 580 (1955).
[8] F. G. Pikus and G. E. Pikus, Phys. Rev. B **51**, 16928 (1995).
[9] W. Knap, C. Skierbiszewski, A. Zduniak, E. Litwin-Staszewska, D. Bertho, F. Kobbi, J. L. Robert, G. E. Pikus, F. G. Pikus, S. V. Iordanskii, V. Mosser, K. Zekentes, and Y. B. Lyanda-Geller, Phys. Rev. B **53**, 3912 (1996).
[10] S. Hikami, A. I. Larkin, and Y. Nagaoka, Prog. Theor. Phys. **63**, 707 (1980).
[11] M. Kohda, V. Lechner, Y. Kunihashi, T. Dollinger, P. Olbrich, C. Schönhuber, I. Caspers, V. V. Bel'kov, L. E. Golub, D. Weiss, K. Richter, J. Nitta, and S. D. Ganichev, Phys. Rev. B **86**, 081306 (2012).
[12] M. Glazov and L. Golub, Semicond. **40**, 1209 (2006).
[13] M. C. Lüffe, J. Kailasvuori, and T. S. Nunner, Phys. Rev. B **84**, 075326 (2011).
[14] N. Averkiev, L. Golub, and G. Pikus, Solid State Commun. **107**, 757 (1998).
[15] I. Garate, J. Sinova, T. Jungwirth, and A. H. MacDonald, Phys. Rev. B **79**, 155207 (2009).
[16] V. Krueckl, M. Wimmer, I. Adagideli, J. Kuipers, and K. Richter, Phys. Rev. Lett. **106**, 146801 (2011).
[17] J. M. Luttinger and W. Kohn, Phys. Rev. **97**, 869 (1955).
[18] R. Winkler, *Spin-Orbit Coupling Effects in Two-Dimensional Electron and Hole Systems* (Springer, Berlin, 2003).
[19] E. I. Rashba and E. Y. Sherman, Phys. Lett. A **129**, 175 (1988).
[20] R. Winkler, H. Noh, E. Tutuc, and M. Shayegan, Phys. Rev. B **65**, 155303 (2002).
[21] D. V. Bulaev and D. Loss, Phys. Rev. Lett. **95**, 076805 (2005).
[22] N. O. Lipari and A. Baldereschi, Phys. Rev. Lett. **25**, 1660 (1970).
[23] P. Wenk *et al.* (unpublished).
[24] X. Bi, P. He, E. M. Hankiewicz, R. Winkler, G. Vignale, and D. Culcer, Phys. Rev. B **88**, 035316 (2013).
[25] A. Scholz, T. Dollinger, P. Wenk, K. Richter, and J. Schliemann, Phys. Rev. B **87**, 085321 (2013).
[26] P. Y. Yu and M. Cardona, *Fundamentals of Semiconductors* (Springer, Berlin, 2010).
[27] V. E. Sacksteder IV and B. A. Bernevig, Phys. Rev. B **89**, 161307(R) (2014).
[28] R. Landauer, IBM J. Res. Dev. **1**, 223 (1957).
[29] M. Büttiker, Y. Imry, R. Landauer, and S. Pinhas, Phys. Rev. B **31**, 6207 (1985).

[30] D. S. Fisher and P. A. Lee, Phys. Rev. B **23**, 6851(R) (1981).
[31] M. Wimmer and K. Richter, J. Comput. Phys. **228**, 8548 (2009).
[32] S. Kettemann, Phys. Rev. Lett. **98**, 176808 (2007).
[33] P. Wenk and S. Kettemann, Phys. Rev. B **81**, 125309 (2010).
[34] L. Landau, Phys. Z. Sov. Union **2**, 46 (1932).
[35] C. Zener, Proc. R. Soc. A **137**, 696 (1932).
[36] C. Betthausen, T. Dollinger, H. Saarikoski, V. Kolkovsky, G. Karczewski, T. Wojtowicz, K. Richter, and D. Weiss, Science **337**, 324 (2012).
[37] O. Zaitsev, D. Frustaglia, and K. Richter, Phys. Rev. B **72**, 155325 (2005).
[38] S. Chakravarty and A. Schmid, Phys. Rep. **140**, 193 (1986).